

Seismic site effects by an optimized 2D BE/FE method

II. Quantification of site effects in two-dimensional sedimentary valleys

B. Gatmiri^{1,2}, C. Arson²

1. University of Tehran, IRAN

2. CERMES, Ecole Nationale des Ponts et Chaussées, Cité Descartes, Champs-sur-Marne, 6-8 avenue Blaise Pascal, 77455 Marne-la-Vallée cedex 2, FRANCE

Tel : (0033) 1 64 15 35 66 or: (0033) 1 64 15 35 24

Fax : (0033) 1 64 15 35 62

gatmiri@cermes.enpc.fr, arson@cermes.enpc.fr

Abstract

This paper deals with the evaluation of seismic site effects due to the local topographical and geotechnical characteristics. The amplification of surface motions is calculated by a numerical method combining finite elements in the near field and boundary elements in the far field (FEM/BEM). The numerical technique is improved by time truncation. In the first part of this article, the accuracy and the relevance of this optimized method are presented. Moreover, parametric studies are done on slopes, ridges and canyons to characterize topographical site effects. The second part deals with sedimentary valleys. The complexity of the combination of geometrical and sedimentary effects is underlined. Extensive parametrical studies are done to

discriminate the topographical and geotechnical effects on seismic ground movement amplifications in two-dimensional irregular configurations. Characteristic coefficients are defined to predict the amplifications of horizontal displacements. The accuracy of this quantitative evaluation technique is tested and discussed.

Key-words

hybrid numerical technique, elastodynamics, site effect, seismic amplification, topography, geotechnical configuration, sedimentary valley, characteristic coefficients, 2D models, predictive calculation method

1. Introduction

As it is stated in [1, 8, 16, 3], the response of a site to a seismic solicitation depends on topography and geotechnical local characteristics. Current building codes [20], based on 1D models of soil columns, do not take 2D phenomena into account to estimate these site effects. An index built on motion intensity is proposed in [26] to evaluate topographical site effects. The following work aims at quantifying the combined effects of geometry and stratigraphy in sedimentary basins subjected to synthetic SV waves of vertical incidence. The main purpose of this paper is to elaborate a predictive method to estimate horizontal ground displacements (u_x) in two-dimensional irregular configurations.

The seismic behaviour of valleys has been studied by many authors, by means of the finite difference method [23], the finite element method [7, 6], the boundary element method [29, 24, 27, 28, 18, 25, 4, 17], and the discrete wavenumber method [15]. The models adopted in this work combine finite elements in the near field and boundary elements in the far field. The simulations are done by means of HYBRID program, developed by Gatmiri and his coworkers [10, 11, 12, 14]. The hybrid numerical technique is optimized by time truncation [9]. The validation of HYBRID and the theoretical aspects of the numerical implementation of the truncation process are presented in the first part of this paper.

In the followings, parametric studies are done on sedimentary basins. Materials are assumed to be dry and linear elastic. The predominant frequency of the incident signal and the impedance contrast between bedrock and sediment are fixed. Taking a reference station on the outcrop, the ratio $u_x/u_{x_{ref}}$ is expressed as a product of

various coefficients. Each factor represents a site effect parameter: offset; sedimentary filling; depth; slope and shape. The topographical and geotechnical variables controlling 2D combined site effects are thus evaluated separately in order to identify the predominant parameters. Specific 2D combined effects are also characterized by a simplified breakdown requiring a unique “2D Combined Amplification” coefficient (2DCA coefficient).

2. Site effects in 2D configurations

2.1. 2D sedimentary effects

In this paragraph, alluvial valleys are studied. The numerical simulations are done with HYBRID program [10]. The main geometrical variables of interest are given on Fig. 1. Rock and sediment behaviours are assumed to be linear elastic. The main parameters are given in Tab. 1. The impedance contrast β is equal to 0.31, where:

$$\beta = \frac{\rho_S \cdot c_S}{\rho_R \cdot c_R} \quad (1)$$

ρ_S and ρ_R are the volumetric masses of sediment and rock, respectively; c_S and c_R are the shear waves velocities of sediment and rock, respectively.

The fundamental resonance frequency of a H -thick sedimentary layer is noted f_{h0} :

$$f_{h0} = \frac{c_S}{4H} \quad (2)$$

2.1.1. 1D and 2D models

Amplification of surface displacements by a sedimentary layer is well-known when the model is one dimensional. It is even possible to characterize the non-linearity of soil [19], or to study exceptional geological configurations [5] by means of 1D-analyses. However, a juxtaposition of soil columns has not the same behaviour as an alluvial valley modelled in two dimensions. Triangular sedimentary valleys subjected to incident SV waves propagating vertically have been studied with the aid of 1D and 2D models in [21].

- duration of 2D seismic responses is lengthened;
- in 1D, the points of the free surface are in phase ; in 2D, there are differential surface horizontal displacements, unless the exciting frequency is equal to the fundamental resonance frequency f_{h0} of the soil column representing the geological layer at the centre of the valley;
- contrary to one-dimensional predictions, a vertical motion is observed at the points located at the surface of a sedimentary valley modelled in two dimensions;
- peak values of displacement amplifications differ, increasing or decreasing depends on the position of the observation point (Fig. 2); generally, 1D amplifications are bigger than 2D ones at low frequencies, and vice versa.

2.1.2. 2D resonance in full sedimentary valleys

The type of resonance of a sedimentary valley is determined by the impedance contrast β and the depth ratio H/L [2] .

If H/L exceeds a critical ratio $(H/L)_c$, incident or reflected volume waves and diffracted surface waves reach the centre of the valley at the same time. 1D vertical resonance of volume waves and lateral propagation of surface waves affect the seismic

response of the site simultaneously. It is impossible to discriminate these two physical phenomena. The valley enters in 2D resonance. 2D fundamental frequencies are given by empirical formulas developed by Bard and Bouchon in [2]:

$$\begin{cases} f_0^P = f_{h0}^P \cdot \sqrt{1 + \left(\frac{H}{L}\right)^2} \\ f_0^{SV} = f_{h0}^{SV} \cdot \sqrt{1 + \left(\frac{2.9 \cdot H}{L}\right)^2} \\ f_0^{SH} = f_{h0}^{SH} \cdot \sqrt{1 + \left(\frac{2 \cdot H}{L}\right)^2} \end{cases} \quad (3)$$

2D fundamental frequencies depend on the nature of the incident wave and the depth ratio H/L - which controls the type of resonance. As a general statement, it can be said that the 2D frequency is higher than the corresponding 1D frequency calculated in a soil column model. Moreover, 2D resonance is characterized by longer seismic responses and by higher maximal motion amplitudes. It is also shown that peak displacement values are reached at higher frequencies than in one dimension, which is in agreement with the observations of Nguyen (paragraph 2.1.1).

2.2. Combination of topographical and geotechnical effects in sedimentary valleys

Topographical and geotechnical effects have been defined separately. In a real sedimentary basin, both aspects affect the seismic response simultaneously. Their superposition can be studied by defining parameters representing the geometrical and stratigraphical characters of the site, such as the shape of the relief, the inclination angle of the slope (α), the normalized depth (H/L) and the filling ratio (H_1/H).

2.2.1. Influence of the exciting frequency and of the impedance contrast

Nguyen studied the influence of the exciting frequency and of the impedance contrast on the response of a full triangular sedimentary valley subjected to SV waves of vertical incidence [21]. In comparison to the case of an empty canyon (part 1 of this paper), the presence of sediments affects the location of peak motion amplitudes considerably.

- The exciting frequency has a weak influence on the duration of the response. At low frequencies (up to $f = f_0$), horizontal displacement amplification reaches a maximum at the centre of the valley and decreases till a minimal value, reached at the edge. In the neighbourhood of the edges, displacements are very similar to the ones at the free surface. At high frequencies ($f > f_0$), the maximum amplification of horizontal displacements is reached off the centre but inside the basin. The temporal response is complex, and there are several surface wave modes.
- f depends on the value of c_s (1), thus on f_{h0} (2), and f_0 (3). That is why observations done at low frequencies (β fixed) are the same as statements claimed for an impedance contrast close to unit (f fixed).

Define the dimensionless frequency η :

$$\eta = \frac{f \cdot L_C}{c} = \frac{L_C}{\lambda} \quad (4)$$

f and λ are the frequency and the wavelength of the signal respectively; c is the wave velocity; L_C is the characteristic dimension of the geometry (for valleys, L_C is the half-width L). As for the empty canyons, site effect gains prominence if the dimensionless frequency η is high.

2.2.2. Influence of the landscape parameters

In the following, interest is focused on parameters characterizing the aspect of the landscape: filling (H_1/H), depth (H/L), inclination angle (α or L_1/L) and shape. Several observation points are studied, in order to evaluate the influence of offset (x/L). In other words, input or mechanical parameters such as the exciting frequency or the impedance contrast are not taken into account.

Sedimentary basins are subjected to an incident Ricker SV wave propagating vertically. Imposed displacements are therefore expressed as:

$$u(t) = A_0 \cdot (a^2 - 0.5) \cdot \exp(-a^2) \quad (5)$$

where:

$$a = \pi \cdot \frac{(t - T_s)}{T_p} \quad (6)$$

Amplification A_0 is fixed to 1; and $T_p = T_s = 0.5s$. The predominant frequency f_C is thus equal to 2 Hz. The incident signal lasts three seconds, but it can be seen from Fig. 3 that amplitude is nearly zero as soon as $t = 1s$. That is why the time window has been defined from $t = 0$ to $t = 3s$. The width of the interval is representative for the study of an eventual lengthening of the seismic response of the site. Displacements are calculated every 0,02 s.

Contrary to the works of Nguyen [21, 13, 22], the influence of landscape parameters is studied in the temporal domain. Maximal values of displacements, calculated in the time interval $[0s;3s]$ are considered. For horizontal displacements, amplifications are normalized by the horizontal displacement at the free surface ($u_x / u_{x_{ref}}$). It is as if the reference station was located on the far outcropping bedrock. At the free surface, vertical displacements are equal to zero. That is why amplification of the vertical

component of the surface ground movement is taken as the absolute value of vertical surface displacements (u_y).

2.2.2.1. Influence of shape

Diverse shapes of basin are studied. Full sedimentary valleys are modelled for the following geometries: triangle, rectangle, ellipse and truncated ellipse ($L_1/L = 0.4$ – Fig. 1).

Some characteristics of the movement amplification are independent from the choice of the shape. Horizontal displacements are systematically amplified at the centre of sedimentary valleys. Amplitude decreases when the observation point is off the centre. At the edge and on the free surface nearby, horizontal displacements are very close to those observed at the free surface (Fig. 4.a and 4.c). The symmetry of the configuration imposes that shear stresses on the axis are equal to zero (i.e. at $x/L = 0$, $\tau = 0$). The continuity of displacements infers that $u_y = 0$ on the axis. Elsewhere, vertical displacements are non-zero. They reach a maximum between $x/L = 0.5$ and $x/L = 0.6$, whatever the geometry of the basin is. At the edge and on the outcrop nearby, the vertical component of surface ground movement varies only slightly (Fig. 4.b and 4.d).

For relieves of same dimensions, the triangular form is the least critical while the rectangular form is the most critical case. Complete and truncated ellipses present an intermediate behaviour and provide very close responses for horizontal and vertical displacements (Fig. 4). Depth increases differences due to shape, and tends to amplify horizontal displacements locally inside the valley, close to the edge (Fig. 4.c).

In a nutshell, statements are the same as for empty canyons (part 1), except that amplification ratios are inversed for horizontal displacements. In a canyon, horizontal motions tend indeed to be attenuated at the centre and slightly amplified at the edge.

On the contrary, in an alluvial basin, horizontal displacements are amplified at the centre and can be locally attenuated near the edge, if depth is large enough.

Elliptic configurations are representative because their behaviour is intermediate. Therefore, influences of depth, inclination angle and filling are mainly presented with the curves of truncated ellipses ($L_1/L = 0.4$).

2.2.2.2. Influence of depth

Depth is one of the parameters controlling embankment. As for the empty canyons (part 1), site effects are reinforced by depth (Fig. 5). When H/L gets greater:

- the amplification of horizontal displacements at the centre increases;
- close to the edge, horizontal displacements reach a local minimum inside the valley (for $x/L \approx 0.8$) and a local maximum at the edge ($x/L = 1$); both local extrema exceed the unit, and are bounded between 1.1 and 1.8;
- the distance from the centre to the point where horizontal displacements are comparable to the ones at the free surface, increases, which means that the zone of influence of the valley becomes wider;
- the peak amplification of vertical displacements gets higher, but the maximum is always located at an off centre point inside the valley ($x/L \approx 0.5$);
- vertical displacements tend to increase outside the alluvial basin when the observation point gets further from the centre; though, it must be kept in mind that on the outcropping bedrock neighbouring the valley, vertical displacements are weak and vary only slightly.

However, vertical displacements are negligible in every configuration for small depths ($H/L = 0.2$).

2.2.2.3. Influence of inclination angle

The influence of the inclination angle α is studied through the variations of the width at the basis L_1 . Tab. 2 sums up the diverse configurations modelled in this parametric study, and the corresponding inclination angles. Fixing the ratio L_1/L to 0,4, it is possible to observe the influence of α through the variations of H/L (Fig. 5). The conclusions are the same as the ones stated for depth (point 2.2.2.2).

2.2.2.4. Influence of filling

Curves representing vertical displacements in function of filling are rather homothetic, except for full valleys ($H_1/H = 1$). As the filling ratio increases, amplification curves of horizontal displacement shift from an “empty canyon behaviour” to “a full valley behaviour”.

For every filling ratio, vertical displacements are negligible on the entire surface of the irregularity if depth is weak ($H/L = 0.2$). In all cases, the vertical component reaches a maximum peak value, for $x/L \approx 0.5$ (Fig. 6.b; 6.d; 6.f and 6.h). Nguyen already observed it on the empty canyons (part 1). This is the only peak for full valleys. For all other filling ratios, a smaller peak value is obtained at the edge ($x/L = 1$). At the edge of partially filled or empty valleys, displacements are calculated at an angular point, generating diffraction phenomena. As soon as the valley is not entirely full, the top of its slope is nude: the irregularity is locally comparable to a mere topographic irregularity. In absence of sediments, the topographical effect induced by slopes generates non-nil vertical displacements (part 1). The presence of a local maximum can be explained by the change of convexity of ellipsoidal geometries at the edge.

Increasing the filling ratio tends to increase peak values of vertical motions and to reinforce horizontal displacement amplifications at the centre of the valley. Horizontal displacements get lower at the edge as filling gets larger (Fig. 6.a and 6.c). These trends correspond to the shift from an “empty-type behaviour” to a “full-type

behaviour". Elliptic configurations are an exception. Inside the valley, horizontal displacements are bigger for the empty canyons than for a filling ratio of 0.25 (Fig. 6.e and 6.g). Horizontal displacements observed at the edge of the empty valleys are the lowest ones among the diverse filling ratios studied. Generally speaking, horizontal amplification curves of the empty elliptic canyons are flat: $u_x/u_{x_{ref}}$ ratio gets from 0.80 at mid-slope to 1.50 at the edge. The variation interval is small compared to the empty truncated ellipse canyons (from 0.65 at the centre to 2.30 at the edge) and to the elliptic 25%-filled valleys (from 0.70 at the centre to 2.20 at the edge). The weak influence of topography in elliptic basins might be explained by the regularity of their shapes, assuming that moderate mean inclination slopes limit topographical site effects. This assumption joins the conclusions of Nguyen (part 1), concerning the criticality of shapes.

At the edge of valleys, horizontal displacements are systematically amplified. At the centre, $u_x/u_{x_{ref}}$ ratio exceeds the unit as soon as the absolute thickness of the sedimentary layer is larger than $0.2 \cdot L$ (Fig. 6.a; 6.c; 6.e and 6.g). This means that central displacements are amplified as soon as the filling ratio H_1/H exceeds a value:

- bounded between 0.5 and 0.75 for $H/L = 0.2$ or 0.4 ;
- bounded between 0.25 and 0.5 for $H/L = 0.6$ or 1 .

In other words, the minimal thickness of the sedimentary layer required to make the geotechnical effect stronger than the topographical effect at the centre of an alluvial basin, is rather weak.

2.2.3. Separation of topographical and geotechnical aspects

It is possible to study combinations of topographical and geotechnical effects by modelling full or partially filled sedimentary valleys. Topographical aspects can be

isolated by focusing on the empty relieves. It is more difficult to separate the geotechnical contribution to site effects in two-dimensional alluvial basins. In this work, 2D geotechnical effects have been characterized through the spatial variations of $u_x(T+G)/u_x(T)$ and $u_y(T+G)/u_y(T)$ ratios, in diverse geometrical configurations of truncated ellipses (Tab. 2). $u_x(T+G)$ and $u_y(T+G)$ are the horizontal and vertical displacements, respectively observed at the surface of a full valley ($H_1/H=1$). $u_x(T)$ and $u_y(T)$ are the horizontal and vertical surface displacements respectively; obtained for the corresponding empty topographies.

For horizontal displacements, 2D geotechnical effects seem to depend on the inclination angle α . Above 31° (Fig. 7.b), repercussions are strong. In the central part of the valley, (from $x/L=0$ to $x/L \approx 0.5$), the presence of sediments amplifies the horizontal displacements characterizing the response of topography. As it could be expected, the maximal amplification is obtained at the centre of the valley, where topographical attenuations and 1D amplifications due to the presence of a sedimentary layer are the more prominent. Between $x/L=0.5$ and $x/L=0.8$, 2D geotechnical effects attenuate horizontal motions. A local maximum is reached at the edge ($x/L=1$). Outside the valley, the 2D geotechnical contribution varies only slightly, and tends to attenuate the horizontal displacement generated by topography. The decreasing geotechnical effect on the outcropping bedrock is logical.

For small inclination angles (Fig. 7.a), the presence of sediments has a very weak influence on horizontal displacements calculated in a two-dimensional topography. The amplification ratio is almost constant inside and outside the valley, with a breaking at the edge. The minimum value in the basin is 0.9, and the maximal amplification on the outcrop is 1.05 (rather negligible). The curve is flat. The modification of the

response by 2D geotechnical effects adds up to a maximum of 10% of the topographical contribution.

Tab. 3 discriminates the cases depending on their sensitivity to 2D geotechnical effects. *Italic characters* correspond to small inclination angles, thus to weak geotechnical contributions. **Bold characters** correspond to steep slopes, thus to a strong influence of the sedimentary layer. Two configurations rise as exceptions. For $(H/L = 1; L_1/L = 0)$ and $(H/L = 0.2; L_1/L = 1)$, inclination angles are huge (45° and 90° respectively), but 2D geotechnical effects are weak (Fig. 7.a). Although the configuration $(H/L = 0.2; L_1/L = 1)$ is rectangular, the small depth of the basin reduces embankment. In its central part, the valley can be modelled by a juxtaposition of 1D soil columns. Geotechnical effects are very similar to the ones provided by 1D models, and are thus weaker than in 2D. Topographical effects exceed 2D geotechnical effects due to a lack of sedimentary influence. It might be the inverse explanation for the case $(H/L = 1; L_1/L = 0)$. Embankment reinforces topographical effects, thus exceeding 2D geotechnical effects.

Discrimination is less clear for vertical displacements. When the valley is deep and steep ($L_1/L = 0; H/L \geq 0.4$) or when the slope is steep ($L_1/L = 1$), topographical effects are huge, and tend to be predominant. The curve representing $u_y(T+G)/u_y(T)$ ratio is flat. In most cases, 2D geotechnical effects even attenuate vertical motions originated by diffraction on the angular points of the relief (Fig. 8.a). In truncated valleys, site effects are mainly due to the influence of the sedimentary layer. The general trend of the curves inside the basin is a geotechnical amplification at the centre, and a regular decreasing from $x/L = 0$ to $x/L = 1$. Vertical displacements are attenuated at the edge, where the $u_y(T+G)/u_y(T)$ ratio reaches a minimum (Fig. 8.b). On the outcrop, a peak value can be obtained for $x/L \approx 1.2$. In these cases, the

amplitude of the vertical component is doubled. Further from the centre, the $u_y(T+G)/u_y(T)$ ratio generally tends to the unit, which means that geotechnical characters have no more influence on the outcropping bedrock. Two configurations are exceptional: $(H/L = 0.2; L_1/L = 0)$ and $(H/L = 0.6; L_1/L = 1)$ cases are sensitive to 2D geotechnical effects (Fig. 8.b). In particular, the valley characterized by $(H/L = 0.2; L_1/L = 0)$ presents a strong geotechnical amplification of vertical displacements for $x/L = 1.2$: the ratio rises to 8. It should also be noted that the trend of the curve representing $(H/L = 0.2; L_1/L = 0.4)$ combination is not common: amplification is huge at the centre (up to 5), and the $u_y(T+G)/u_y(T)$ ratio is almost nil elsewhere.

3. Characterization and quantification of the amplification of horizontal surface displacements in 2D sedimentary valleys

As shown in subparagraph 2.2.3, it is not easy to discriminate topographical and 2D geotechnical effects affecting the seismic response of an alluvial valley. It is though an important issue in engineering. In this part, a method of prediction of horizontal displacements is exposed. The aim of this technique is to evaluate amplifications of the horizontal component of ground movement without using numerical simulations. Displacement amplification is defined as $u_x/u_{x_{ref}}$ (See subparagraph 2.2.2), where $u_{x_{ref}}$ is the horizontal displacement observed at the surface of a half-space made of

rock. The incident signal is a Ricker SV wave propagating vertically (See (5), (6) and Fig. 3). Materials are assumed to be dry and linear elastic (See Tab. 1). The main geometrical parameters are defined on Fig. 1. Two shapes are studied for the alluvial basin: trapeziums (for $H_1/H = 0;1$) and truncated ellipses (for $H_1/H = 0;0.25;0.5;0.75;1$). ($H/L; L_1/L$) combinations chosen for the study are summed up in Tab. 2. The present work only deals with observation points located in the basin. The response of the neighbouring outcrop is not studied.

3.1. Expression of displacement amplifications as a product of characteristic coefficients

Topographical and geotechnical conditions, that contribute to horizontal ground motion amplification, are separated by means of five significant coefficients. Factors represent the influence of parameters controlling site effects: offset (x/L); filling (H_1/H); depth (H/L); inclination angle of the slope (α) and shape of the basin (trapezium or truncated ellipse).

$$\frac{ux}{ux_{ref}} = \frac{ux^*(0, -(H - H_1))}{ux^*(0, -(H - H_1))} \cdot \frac{ux^*(0, -(H - H_1))}{ux^*(0, -H)} \cdot \frac{ux^*(0, -H)}{ux^*(L, 0)} \cdot \frac{ux^*(L, 0)}{ux^*(L_1, -H)} \cdot \left[\frac{ux}{ux^*(L_1, -H)} \cdot \frac{ux^*(L_1, -H)}{ux_{ref}} \right] \quad (7)$$

- Offset coefficient:

$$\frac{ux^*(0, -(H - H_1))}{ux^*(0, -(H - H_1))} = f(x/L; H_1/H) \quad (8)$$

- Filling coefficient:

$$\frac{ux^*(0, -(H - H_1))}{ux^*(0, -H)} = f(H_1 / H) \quad (9)$$

- Depth coefficient:

$$\frac{ux^*(0, -H)}{ux^*(L, 0)} = f(H / L) \quad (10)$$

- Slope coefficient:

$$\frac{ux^*(L, 0)}{ux^*(L_1, -H)} = f(\alpha) \quad (11)$$

- Shape coefficient:

$$\frac{ux}{ux^*} \cdot \frac{ux^*(L_1, -H)}{ux_{ref}} = f(\text{shape}; x / L; H / L) \quad (12)$$

Offset, filling, depth and slope coefficients are assumed to be independent from the shape of the topography. These four ratios are calculated on truncated ellipses and applied to every configuration. That is why they are marked with *. The correction is done through the shape factor. The shape factor is equal to one for truncated ellipses, and must be calculated from formula (12) in other cases. If $L_1 / L = 1$, the valley is rectangular whatever the chosen basin shape is. Offset, filling, depth and slope coefficients are always equal to the ones obtained for truncated ellipses. The shape coefficient can be considered one, and another assumption is not necessary. For other values of L_1 / L , ellipsoidal configurations give intermediate responses for both empty and full valleys (Fig. 16 of part 1; Fig.4), which makes them representative.

Variables controlling filling, depth and slope have been separated, so the corresponding coefficients depend on only one parameter (9; 10 and 11). For a given abscissa x / L , the filling ratio H_1 / H determines the type of material on which the superficial observation point is located. That is why the offset coefficient does not only depend on x / L , but also on H_1 / H parameter, which introduces a second dimension

in the definition of the geometrical location of the observation point. The shape coefficient varies with three geometrical parameters, in order to make it representative of the influence of the curvature of the slope.

3.1.1. Offset coefficient

Horizontal displacements are calculated on regularly spaced points at the surface of ellipsoidal basins. For each filling ratio H_1/H , the maximal value obtained for the offset coefficient (8) among all the $(H/L; L_1/L)$ combinations is retained (See Tab.2). Fig. 9 represents the corresponding curves.

If the valley is full ($H_1/H = 1$), the horizontal surface displacement reaches a maximum at the centre of the basin. That is why offset is an attenuation factor. Partially filled valleys manifest a topographical effect on the top part of the slope. It tends to amplify horizontal displacements. The width of the domain submitted to topographical effects increases as filling decreases. Offset is thus an amplification factor. Amplification rises if the sedimentary layer is thin or if x/L is close to one. At the edge, the offset ratio is equal to 1.8 if $H_1/H = 50\%$ and to 3.7 if $H_1/H = 25\%$. The biggest offset ratios are obtained for $H_1/H = 25\%$, and not for $H_1/H = 0\%$, as could be expected. In fact, it was already observed in subparagraph 2.2.2.4 that in elliptic valleys ($L_1/L = 0$), site effects could be “more topographic” in the $H_1/H = 25\%$ case than in the $H_1/H = 0\%$ case (Fig. 6). Considering the way the offset coefficient has been built, this means that the biggest offset effects occur in elliptic valleys. Truncating the shape attenuates the phenomenon.

3.1.2. Filling coefficient

As for the offset ratio, the filling coefficient (9) is calculated in every configuration, and for a fixed filling ratio H_1/H , the maximal value obtained among all the $(H/L; L_1/L)$ combinations is retained. Fig. 10 represents the corresponding graph.

The filling coefficient represents a mere 1D geotechnical effect. Without damping, calculations at the resonance of a soil column yield to a maximal amplification of horizontal displacements reaching $1/\beta$, where β is the impedance ratio (1). In our models, $\beta = 0.31$, so the maximal amplification expected is 3.22. This threshold is never reached. Consequently, the soil column located at the centre of the basin never enters in 1D resonance. 1D fundamental frequencies f_{h0} (2), calculated for every configuration, are given in Tab. 4.

The configurations in which the predominant frequency of the incident signal ($f_C = 2\text{Hz}$) is the closest to the 1D fundamental frequency correspond to the most filled valleys. Due to the position relative to the amplification peak at resonance, basins with high filling ratios are thus more susceptible to amplify central horizontal displacements. This induces larger filling coefficients. This statement explains why the filling coefficient increases with the filling ratio H_1/H (Fig. 10). In all cases, the filling coefficient is an amplification factor.

3.1.3. Depth coefficient

The calculation method is similar to the one of the filling coefficient. The depth coefficient (10) is calculated in every configuration. For each value of H/L , the maximal value obtained among all the $(L_1/L; H_1/H)$ combinations is retained. The depth coefficient is defined as the ratio of horizontal displacements calculated on a point of substratum to horizontal displacements calculated at the edge of the valley.

However, section 2 showed that surface displacement increased with depth. To study depth effects, it is thus more natural to study horizontal displacements on a point of the surface relative to those at a point of substratum. That is why Fig. 11 represents the inversed depth coefficient.

It has been shown in subparagraph 2.2.2.4 (Fig. 6) that amplification of surface displacements rose with the absolute thickness of the sedimentary layer. The inverse depth coefficient increases with depth, which is in agreement with this statement. Moreover, horizontal displacements calculated at the edge of valleys are systematically amplified. It could thus be expected that the inversed depth coefficient would be more than unit. As a consequence, the inverse coefficient is always an amplification factor. This means that in the decomposition (7), the depth coefficient is an attenuation factor.

3.1.4. Slope coefficient

For a given inclination angle α , the maximal slope coefficient (11) calculated for the whole ($H/L; L_1/L; H_1/H$) combinations is retained. The curve is shown on Fig. 12.

In the construction of the slope coefficient (11), geotechnical effects vanish due to the maximization on α . Overestimation of slope amplification rises to a maximum of 2.3 times the amplifications calculated by numerical simulation. The scale of order is thus preserved. This means that the slope coefficient really represents a mere topographical aspect of site effects. Parametric studies done on the empty canyons (Fig. 14 of part 1) showed that displacement amplifications got stronger as the slope became steeper. The increase of the slope coefficient with α reflects this trend (Fig. 12).

Topographical effects are mainly caused by:

- wave focusing in convex relieves;

- interferences between incident and reflected volume waves with diffracted surface waves.

If embankment is low, surface waves get late relatively to volume waves. Interferences have thus less chance to occur. Moreover, convexity rises with depth and steep-sidedness, thus with α .

In other words, an increase of the slope coefficient is expected when:

- increases;
- H/L increases at a fixed value of L_1/L ;
- L_1/L decreases at a given value of H/L .

The last two statements can explain why the increasing of the slope coefficient is not monotonous. Indeed, the coefficient is weaker for 34° than for 31° . In the parametric study (See Tab. 2), the 31° inclination angle corresponds to the ($H/L = 0.6; L_1/L = 0$) configuration, and the 34° angle refers to ($H/L = 0.4; L_1/L = 0.4$). Both angles are very close. The determining parameter is thus the width at the base of the valley (L_1). In the ($H/L = 0.4; L_1/L = 0.4$) configuration, the slope is steeper, but the opening at the base works against the expected amplification.

As recalled for the depth coefficient, horizontal displacements at the edge of valleys are always amplified. Therefore, it is not surprising to find that the slope coefficient is more than unit (See (11)). For all cases, the slope coefficient is thus an amplification factor.

3.1.5. Shape coefficient

In this parametric study, only one shape coefficient has been considered, since only one shape has been modelled in addition to the ellipsoidal reference configuration (See

(12)). Shape represents a mere topographical effect. That is why the determination of the shape coefficient is based on the comparison of empty trapezoidal and ellipsoidal canyons of the same dimensions (for H/L and L_1/L). Only the horizontal displacements calculated for $L_1/L = 0.4$ are used for the calculation. In other words, H_1/H and L_1/L are fixed. The shape coefficient depends only on x/L and H/L . To find out u_x/u_x^* , displacements are evaluated on regularly spaced observation points at the surface of both canyons. The resulting graphs are given on Fig. 13.

Variations of the shape coefficient increase with depth. Shifting from an ellipsoidal configuration to a trapezoidal shape induces an attenuation of horizontal surface displacements. The attenuation is minimal at the centre (about 0.8) and maximal at the edge (down to the half of the amplifications obtained for truncated ellipses).

3.2. Simplification of the breakdown: a unique “2D Combined Amplification” coefficient (2DCA coefficient)

Calculations on 1D site effects are mastered. Paragraph 3.1 presents a predictive evaluation method of horizontal displacements for 2D models. This paragraph aims at developing a simplified technique based on a unique “2D Combined Amplification” coefficient (2DCA coefficient). It is assumed that horizontal displacement at the centre of the valley is known. In engineering problems, this is generally the case. $u_x(0, -(H - H_1)) / u_x(0, -H)$ can indeed be evaluated by means of a 1D column model with moderate errors. The objective is to build a coefficient that could sum up the influence of the second dimension in the model. 1D models are based on vertical analyses. That is why the 2DCA coefficient must depend on x/L . The offset

coefficient (8) meets this condition. As for the preceding breakdown (7), it is assumed that ellipsoidal configurations could be set as references. Consequently, the offset coefficient must be corrected by the shape coefficient (12). The resulting simplified breakdown is thus expressed as:

$$\frac{u_x}{u_{x_{ref}}} = \frac{u_x^*(0, -(H - H_1))}{u_x^*(0, -H)} \cdot \frac{u_x^*}{u_x^*(0, -(H - H_1))} \cdot \left[\frac{u_x}{u_x^*} \cdot \frac{u_x^*(L_1, -H)}{u_{x_{ref}}} \right] \quad (13)$$

- 1D amplification ratio:

$$\frac{u_x^*(0, -(H - H_1))}{u_x^*(0, -H)} \quad (14)$$

- 2DCA coefficient:

$$\frac{u_x^*}{u_x^*(0, -(H - H_1))} \cdot \left[\frac{u_x}{u_x^*} \cdot \frac{u_x^*(L_1, -H)}{u_{x_{ref}}} \right] = f(x/L; H_1/H; H/L; \text{shape}) \quad (15)$$

Comparing the two decompositions (7) and (13), it can be seen that the simplification consists in eliminating the depth and slope coefficients, and to replace the reference filling coefficient (8) by an exact filling coefficient representing 1D effects (14). For truncated ellipses, the shape coefficient is equal to unit, so that the “2D Combined Amplification” coefficient (2DCA coefficient) is similar to the offset coefficient (Fig. 9). For trapezoidal valleys, the aspect of the 2DCA coefficient curve strongly depends on the filling ratio H_1/H (Fig. 14). For empty canyons, the 2DCA coefficient is an amplification factor, increasing with offset (from 1 at $x/L = 0$ to 3 at $x/L = 1$). For full sedimentary valleys, it is an attenuation factor, varying only slightly with x/L (regularly decreasing from 0.8 at the centre to a minimum of 0.5 at the edge).

3.3. Relevance and accuracy of the breakdowns

Amplifications of horizontal displacements are calculated by three methods: numerical simulation, product of five coefficients (7), and expression using a single 2DCA coefficient (13). Results obtained through breakdowns are compared to those given by HYBRID:

$$\frac{\left(\frac{u_x}{u_{x_{ref}}}\right)_{\text{predictive}}}{\left(\frac{u_x}{u_{x_{ref}}}\right)_{\text{numerical}}} \quad (16)$$

The product of five factors (7) involves maximized ratios. Amplification is thus systematically over-estimated. In the simplified technique (13), the 1D amplification factor corresponds to an exact value. Moreover, the 2DCA coefficient can be attenuating for full valleys (Fig. 9 for truncated ellipses and Fig. 14.b for trapeziums). Therefore, the 2DCA coefficient method may lead to under-estimations. The performances of both predictive calculation methods are studied through:

- a comparison of over-estimations of $u_x / u_{x_{ref}}$ (Fig. 15 and 16);
- an evaluation of the under-estimation risks in the breakdown using the 2DCA coefficient (Fig. 17 and 18).

Over-estimations provided by the 5-factor breakdown are systematically higher than the ones given by the 2D-coefficient method. It is normal, since in the first product (7), over-estimations are summed in five ratios, whereas the simplified technique (13) requires only three factors. The largest over-estimations deal with shallow rectangular valleys ($H/L = 0.2$ or 0.4 ; $L_1/L = 1$). The absolute error (16) rises up to 14 for truncated ellipses, and to 9 for trapeziums. Errors are greater on empty or poorly filled valleys ($H_1/H = 0$ or 0.25). The absolute error adds up to about 4 for the 5-factor breakdown applied on truncated ellipses, whereas it is between 2 and 3 through the 2DCA coefficient method (Fig. 15.a and 15.b). In trapezoidal valleys, the error is about 3 with the 5-factor technique and 2 with the simplified method (Fig.16.a). When the

sedimentary layer is thick ($H_1/H = 0.75$ or 1), the 2D-coefficient technique is really more precise: the absolute error (16) is very close to unit. On the contrary, the product of five factors over-estimates amplifications from 3 to 5 times in most cases (Fig. 15.d; 15.e and 16.b). Both techniques give the same accuracy on half-filled ellipsoidal valleys (Fig. 15.c).

The 2DCA coefficient evaluation technique is not so hazardous. Truncated elliptic valleys present no risk of horizontal displacement under-estimations (Fig. 17). For trapezoidal valleys, risks are nil for the empty canyons, and weak for the full valleys: the minimal absolute error (16) reaches to 0.85 (Fig. 18). An exception is the deep empty rectangle ($H/L = 1; L_1/L = 1; H_1/H = 0$), for which the 2DCA coefficient predictive method evaluates horizontal displacement amplification to 60% of its value.

As a conclusion, the 2DCA coefficient (15) is relevant to estimate amplifications of horizontal displacements due to site effects. Over-estimations scarcely exceed twice the value calculated by a numerical method. Risks of under-estimations are not so significant. It is possible to get a good approximation of amplifications by applying a security coefficient of about 1.25. Though, the physical interpretation of the 2DCA coefficient must be considered cautiously. In fact, amplification ratio (14) does not represent mere 1D effects, because it is calculated on the base of a 2D calculation. In strongly embanked valleys, topographical and 2D basin effects affect the response of the site at the centre. Consequently, the 2DCA coefficient (15) does not sum up the entire physical phenomena induced by 2D configurations. The main advantage of the 5-factor breakdown (7) is that each aspect of 2D site effects is separated from the other, which can provide some physical explanations. Huge over-estimations are stated, but the accuracy of the five coefficients can be improved by using appropriate optimization techniques. In this study, offset, filling, depth, slope and shape effects are

quantified through rough maximizations. Correlations based on a statistical study could bring interesting improvements.

4. Conclusion

Site effects have been studied by means of a hybrid numerical technique optimized by time-truncation (part 1). Several parametric studies have been done with HYBRID program, in order to characterize the combined effects of topographical irregularities and sedimentary filling on ground motion.

Statements concerning the influences of depth, inclination slope angle and shape in the alluvial valleys are the same as for the empty canyons, except that amplification ratios are inversed for horizontal motions. In a canyon, horizontal displacements tend indeed to be attenuated at the centre and slightly amplified at the edge. On the contrary, in an alluvial basin, horizontal displacements are amplified at the centre and can be locally attenuated near the edge if depth is large enough. Geotechnical effects tend to dominate topographical effects as soon as the thickness of the sedimentary layer exceeds $0.2 \cdot L$.

Geotechnical effects are well-known in one dimensional models. A qualitative comparison between seismic responses of the empty and full valleys has shown that 2D geotechnical effects increased with depth and steep-sidedness. In the central part of valleys, the presence of sediments amplifies horizontal motions characterizing the response of topography. A local maximum is reached at the edge. Outside the valley,

the 2D geotechnical contribution varies only slightly, and tends to attenuate the horizontal displacement generated by topography.

In engineering problems, it is useful to predict motion amplifications without using numerical simulation. Two evaluation techniques have been developed. A breakdown of horizontal surface displacement amplification in five factors describes qualitatively and quantitatively the contributions of different parameters controlling site effects (offset, filling, depth, slope, shape). Amplifications can be hugely over-estimated. A “2D Combined Amplification” coefficient (2DCA coefficient) is defined to simplify the breakdown technique. This gives better quantitative results, and risks of amplification under-estimations are weak.

Statistical post-treatment of data can improve the accuracy of the calculation methods developed to evaluate the amplification of horizontal motions in two-dimensional irregular configurations. Other terms could be included in the breakdown, such as an exciting frequency ratio controlling the resonance type of the valley, or a mechanical coefficient related to the impedance contrast. Moreover, applications in engineering must be based on simulations done with real seismic input signals. Hopefully the results could be used in microzonation or in paraseismic norms.

Acknowledgements

This paper states the main results obtained with HYBRID program. Some of results are reported from the PhD dissertation of KV Nguyen [21].

Appendix

c	wave velocity
c_R	shear wave velocity of rock
c_S	shear wave velocity of sediment
f	frequency of the input signal
f_0	fundamental resonance frequency of a sedimentary valley modeled in two dimensions
f_c	predominant frequency of an incident Ricker input signal
f_{h0}	fundamental resonance frequency of a H -thick sedimentary layer
u_x	maximal amplitude of ground displacements in x-direction
$u_{x_{ref}}$	amplitude of horizontal ground displacements at the free surface
$u_x(T)$	maximal amplitude of ground displacements in x-direction at the surface of an empty canyon
$u_x(T+G)$	maximal amplitude of ground displacements in x-direction at the surface of a full valley
u_y	maximal amplitude of ground displacements in y-direction
$u_y(T)$	maximal amplitude of ground displacements in y-direction at the surface of an empty canyon
$u_y(T+G)$	maximal amplitude of ground displacements in y-direction at the surface of a full valley
x	abscissa of the observation point
H	depth of a valley

- H_1 height of the sedimentary layer filling a valley
- L half-width at the surface of a valley
- L_1 half-width at the base of a valley
- L_C characteristic dimension of the geometry: $L_C = H$ for a slope (height), and
 $L_C = L$ for a canyon or a ridge (half-width)
- α characteristic inclination angle of the topography
- β impedance contrast
- η dimensionless frequency
- λ wavelength of the input signal
- ν Poisson's ratio
- ρ volumetric mass

References

- [1] Aki. Local Site Effects On Strong Ground Motion. Earthquake Engineering and Soil Dynamics II : Recent Advances in Ground Motion Evaluation, p 103 – 155, Geotechnical Special Publication, American Society of Civil Engineering, New-York, 1988.
- [2] Bard P-Y, Bouchon M. The two-dimensional resonance of sediment-filled valleys. Bulletin of the seismological society of America 1985; 75(2):519-540.
- [3] Bard P-Y, Riepl-Thomas. In: Wave Motion in Earthquake Engineering, Chapter 2: Wave Propagation in Complex Geological Structures and their Effects on Strong Ground Motion, 37 – 95. WIT Press, 2000.
- [4] Barros, Luco. Amplification of Obliquely Incident Waves by a Cylindrical Valley Embedded in a Layered Half-Space. Earthquake Engineering and Structural Dynamics 1995; 24:163 – 175.
- [5] Bessasson, Kaynia. Site Amplification in Lava Rock on Soft Sediments. Soil Dynamics and Earthquake Engineering 2002; 22:525 – 540.
- [6] Bielak, Xu, Ghattos. Earthquake Ground Motion and Structural Response in Alluvial Valleys. Journal of Geotechnical and Geoenvironmental Engineering 1999.
- [7] Castellani A, Peano A, Sardella L. On analytical and numerical techniques for seismic analysis of topographic irregularities. In: Proc of the 7th European Conference on Earthquake Engineering. Athens, Greece, 1982, 2:415–423.
- [8] Faccioli. Seismic Amplification in the Presence of Geological and Topographic Irregularities. In: Proc of the 2nd International Conference on Recent Advances in Geotechnical Earthquakes Engineering and Soil Dynamics. 1991.

- [9] Gatmiri B, Dehghan K. Applying a new fast numerical method to elasto-dynamic transient kernels in HYBRID wave propagation analysis. In: Proc of the 6th Conference on Structural Dynamics (EURODYN 2005). Paris, France, 2005, Millpress, Rotterdam, 1879-1884.
- [10] Gatmiri B, Kamalian M. Two-Dimensional transient Wave Propagation in Anelastic Saturated Porous Media by a Hybrid FE/BE Method. In: Proc of the 5th European Conference of Numerical Methods in Geotechnical Engineering. Paris, France, 2002, 947-956.
- [11] Gatmiri B, Kamalian M. On the fundamental solution of dynamic poroelastic boundary integral equations in the time domain. International Journal of Geomechanics 2002; 2(4):381-398.
- [12] Gatmiri B, Nguyen KV. Time 2D Fundamental solution for Saturated Porous Media with Incompressible Fluid. International Journal of Communications in Numerical Methods in Engineering 2005; 21:119-132.
- [13] Gatmiri B, Nguyen KV; Dehghan K. Seismic Response of Slopes subjected to incident SV Wave by an Improved Boundary Element Approach. Accepted for publication in International Journal for Numerical and Analytical Methods in Geomechanics.
- [14] Kamalian M, Jafari MK, Sohrabi-Bidar A, Razmkhah A, Gatmiri B. Time-Domain Two-Dimensional Site Response Analysis of Non-Homogeneous Topographic Structures by A Hybrid FE/BE Method. International Journal of Soil Dynamics and Earthquake Engineering 2006; 26(8):753-765.
- [15] Kawase H. Time-domain response of a semicircular canyon for incident SV, P and Rayleigh waves calculated by the discrete wavenumber boundary element method. Bulletin of the seismological Society of America 1988; 78:1415-1437.

- [16] Lacave, Bard, Koller. Microzonation: Techniques and Examples. In: Block 15: Naturgefahren - Erdbebenrisiko, 23-pages-article published on: www.ndk.ethz.ch/pages/publ/Koller.pdf, 1999.
- [17] Luco, Barros. 3D Response of a Layered Cylindrical Valley Embedded in a Layered Half-Space. *Earthquake Engineering and Structural Dynamics* 1995; 24:109 – 125.
- [18] Luco, Wong, Barros. 3D Response of a Cylindrical Canyon in a Layered Half-Space. *Earthquake Engineering and Structural Dynamics* 1990; 19:799–817.
- [19] Lussou, Bard, Modaressi, Gariel. Quantification of Soil Non-Linearity based on Simulation. *Soil Dynamics and Earthquake Engineering* 2000; 20:509 – 516.
- [20] Martin, Dobry. Earthquake Site Response and Seismic Code Previsions. *NCEER Bulletin* 1994; 8(4).
- [21] Nguyen KV. Etude des effets de site dûs aux conditions topographiques et géotechniques par une méthode hybride éléments finis / éléments frontières, PhD dissertation, Ecole Nationale des Ponts et Chaussées, 2005. (in French)
- [22] Nguyen KV, Gatmiri B. Evaluation of seismic ground motion induced by topographic irregularities. Accepted for publication in *International Journal of Soil Dynamics and Earthquake Engineering*.
- [23] Ohtsuki, Karumi. Effects of Topography and Subsurface Inhomogeneities on Seismic SV Waves. *Earthquake Engineering and Structural Dynamics* 1983; 11:441 – 462.
- [24] Sanchez-Sesma FJ. Ground motion amplification due to canyons of arbitrary shape. In *Proc of the 2nd International Conference on Microzonation*. San Francisco, California, 1978, 729-738.

- [25] Sanchez-Sesma FJ, Campillo M. Diffraction of P, SV and Rayleigh waves by topographic features: A boundary integral formulation. *Bulletin of the seismological Society of America* 1991; 81(6): 2234-2253.
- [26] Sanchez-Sesma, Faccioli, Fregonese. An Index for Measuring the Effects of Topography on Seismic Ground Motion Intensity. *Earthquake Engineering and Structural Dynamics* 1986; 14:719 – 731.
- [27] Sanchez-Sesma FJ, Herrera I, Aviles J. A boundary method for elastic wave diffraction: application to scattering waves by surface irregularities. *Bulletin of the seismological Society of America* 1982; 72:473-490.
- [28] Vogt RF, Wolf JP, Bachmann H. Wave scattering by a canyon of arbitrary shape in a layered half-space. *Earthquake Engineering and Structural Dynamics* 1988; 16:803-812.
- [29] Wong H, Jennings P. Effect of canyon topographies on strong ground motion. *Bulletin of the seismological Society of America* 1975; 65:1239–1257.

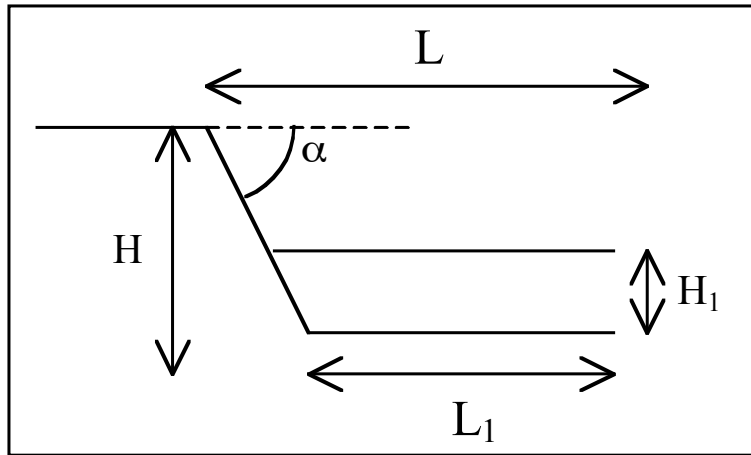
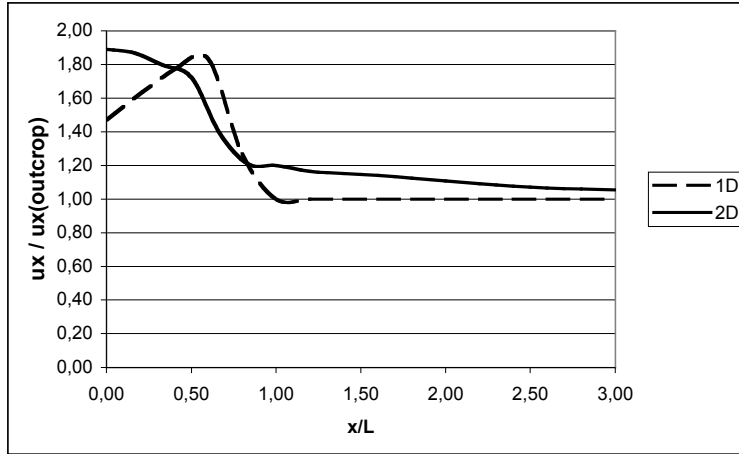


Figure 1: Main geometrical parameters characterizing the alluvial basins. Due to symmetry, only the half of the valley is represented.



**Figure 2: Comparison of 1D and 2D models – Triangular full sedimentary valley,
 $H/L = 1$.**

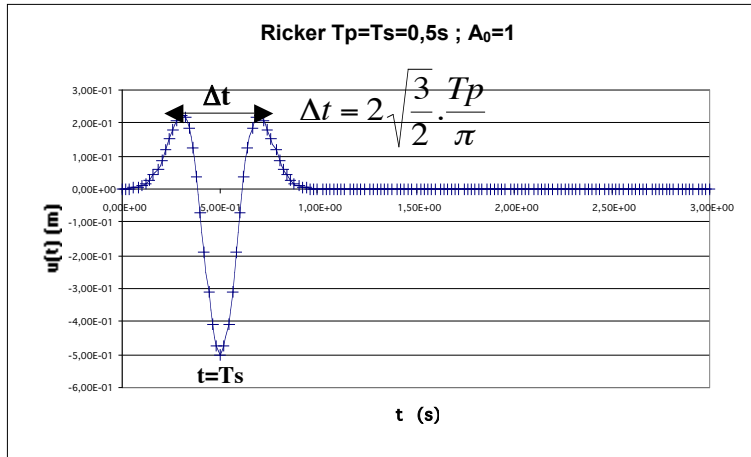
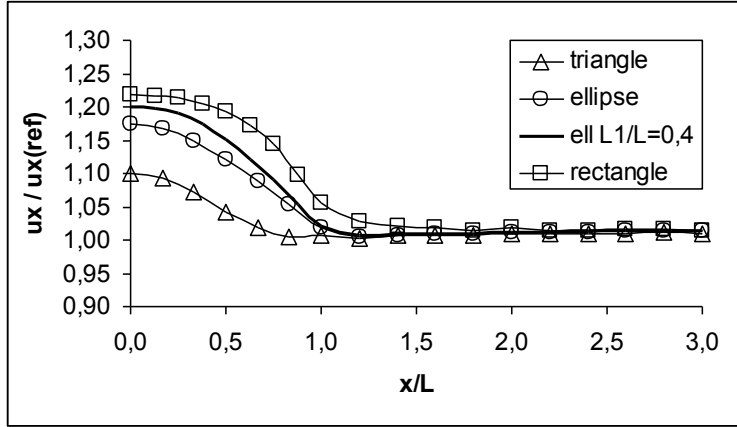
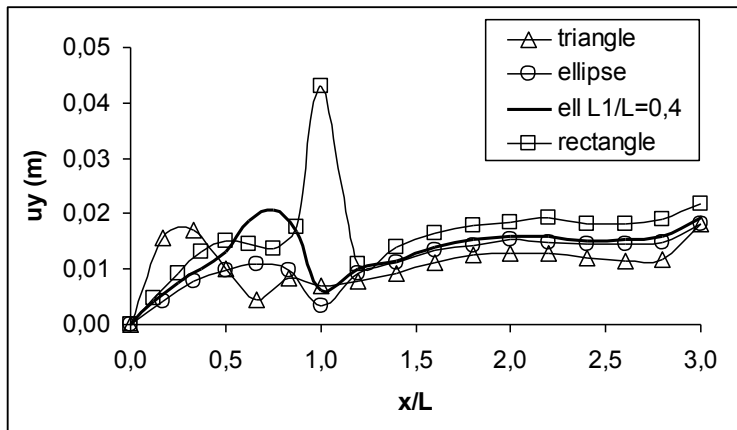


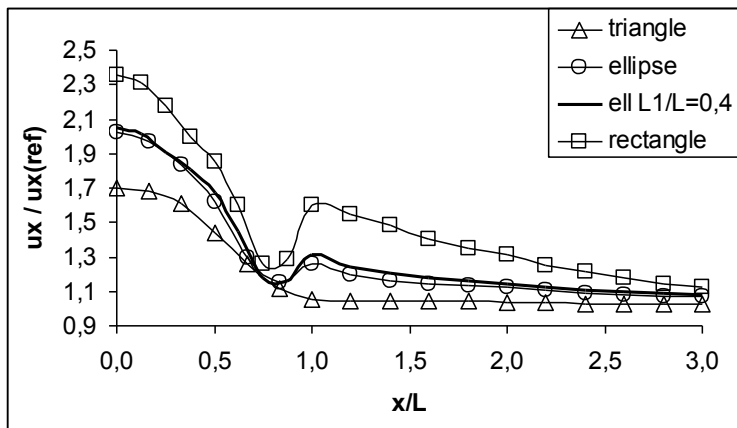
Figure 3: Incident Ricker signal



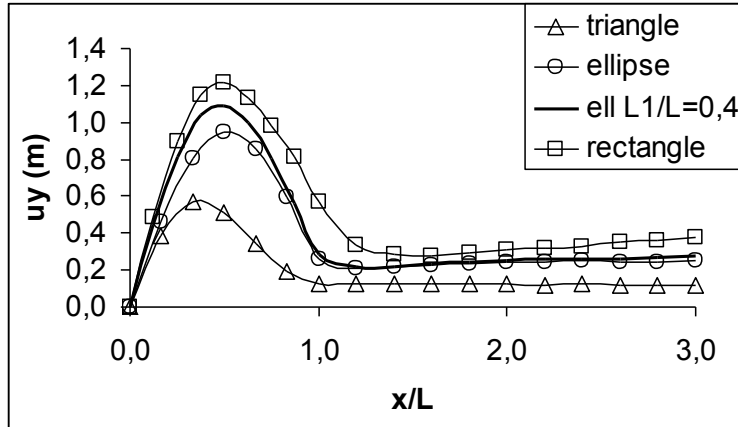
a. u_x , $H/L = 0.2$



b. u_y , $H/L = 0.2$

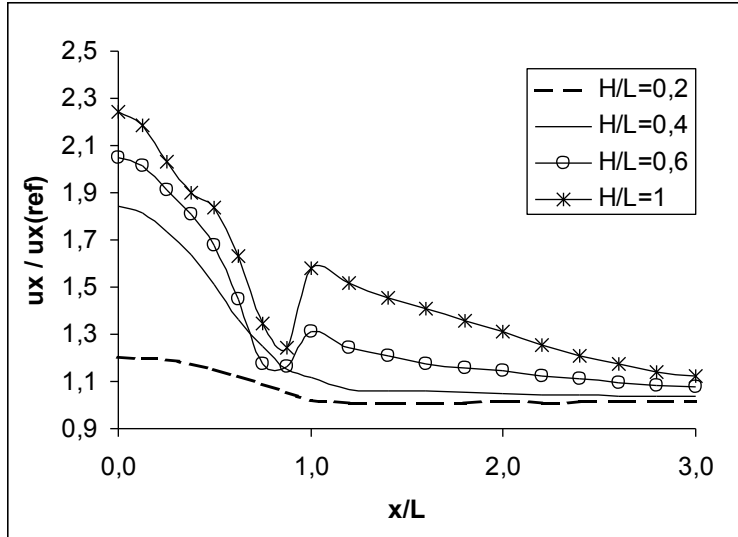


c. u_x , $H/L = 0.6$

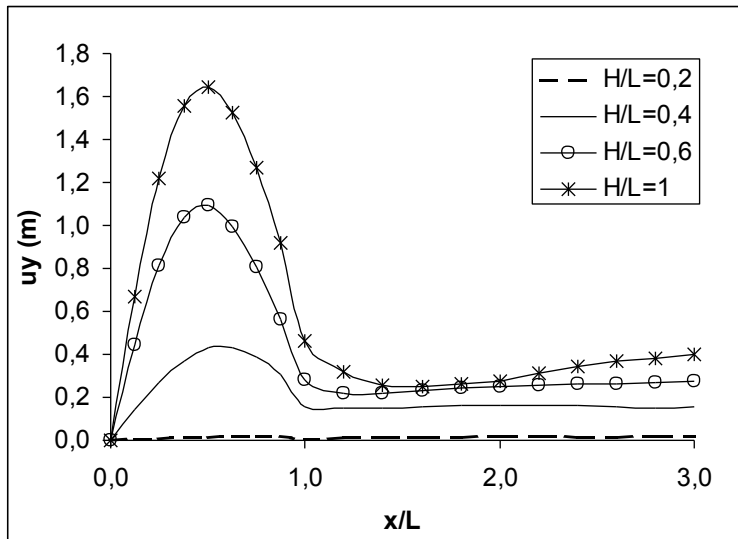


d. u_y , $H/L = 0.6$

Figure 4: Influence of shape on horizontal (a; c) and vertical (b; d) displacements at the surface of full alluvial valleys: $H/L = 0.2$ (a; b) and $H/L = 0.6$ (c; d)

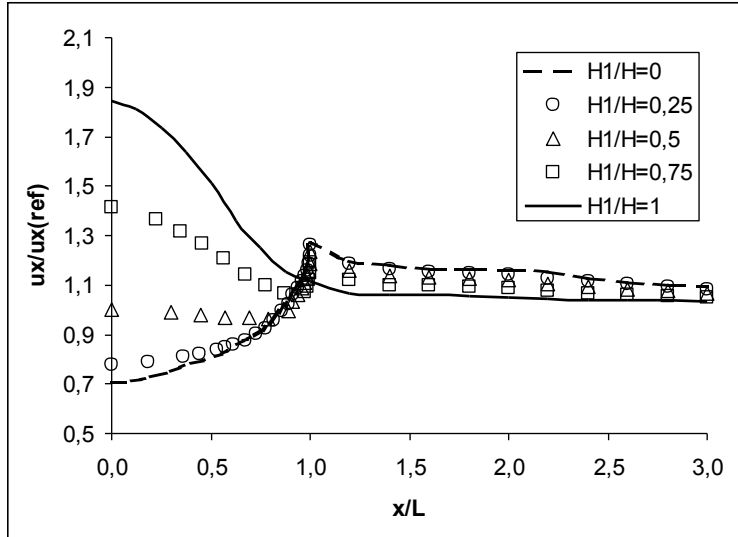


a. Horizontal amplification

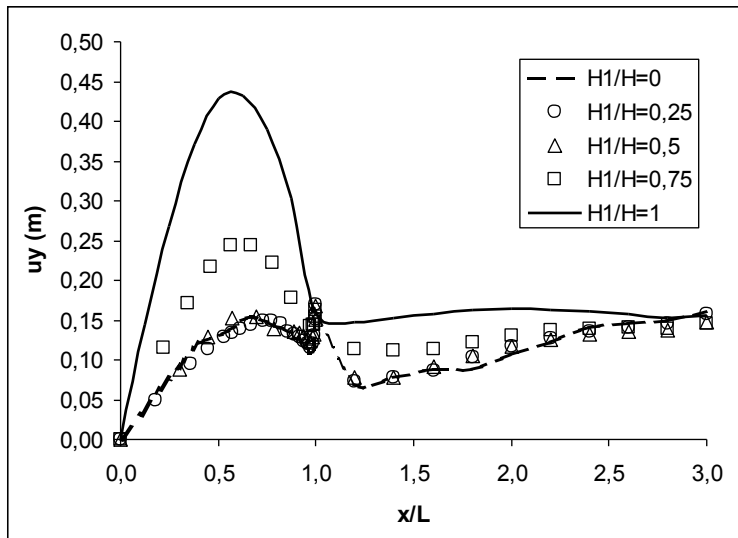


b. Vertical displacements

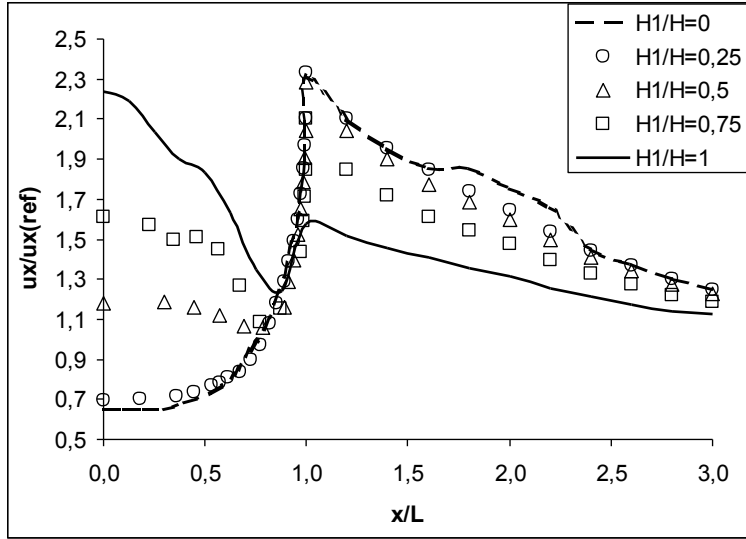
Figure 5: Influence of depth on the response of full sedimentary valleys - truncated ellipses, $L_1/L = 0.4$



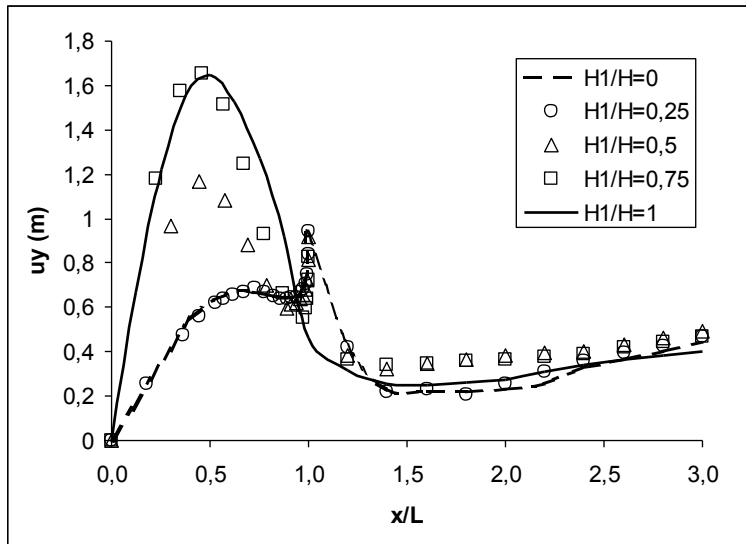
a. u_x , $H/L = 0.4$, $L_1/L = 0.4$



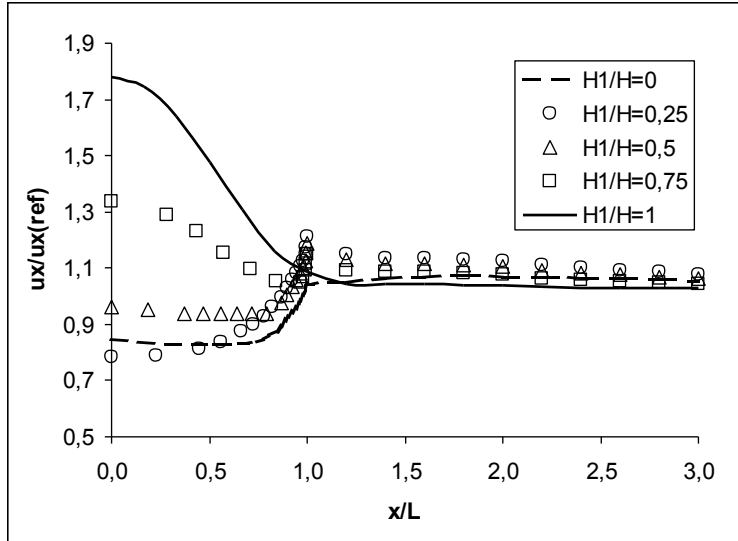
b. u_y , $H/L = 0.4$, $L_1/L = 0.4$



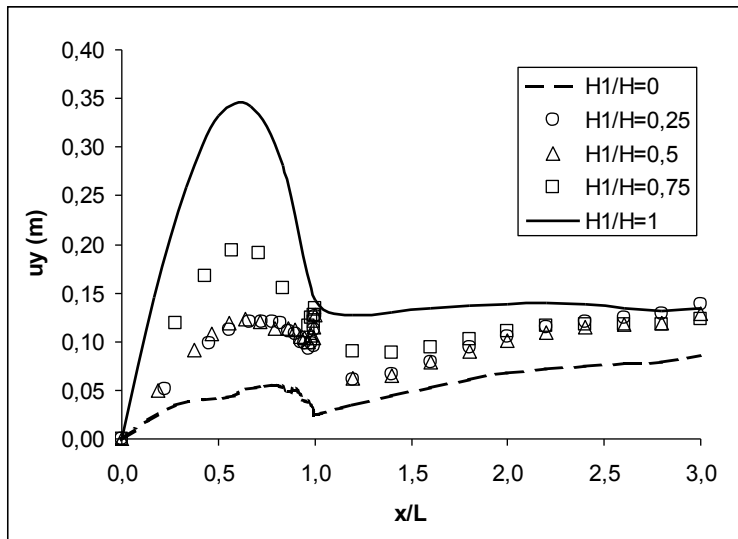
c. u_x , $H/L = 1$, $L_1/L = 0.4$



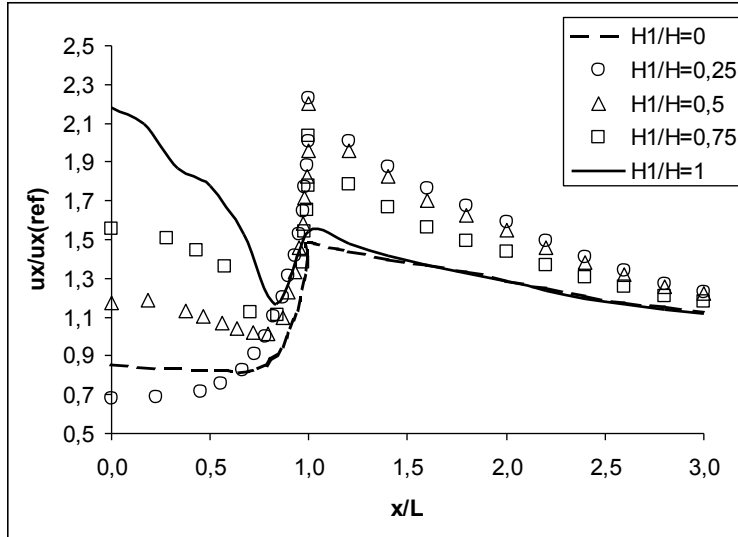
d. u_y , $H/L = 1$, $L_1/L = 0.4$



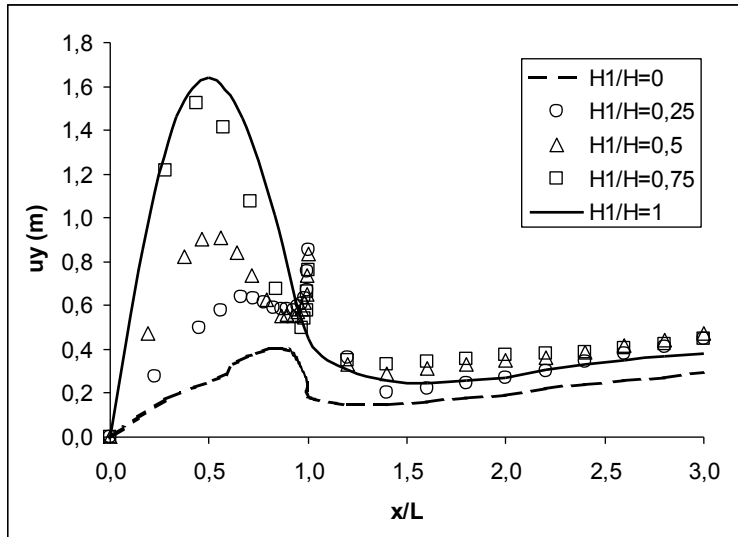
e. u_x , $H/L = 0.4$, $L_1/L = 0$



f. u_y , $H/L = 0.4$, $L_1/L = 0$

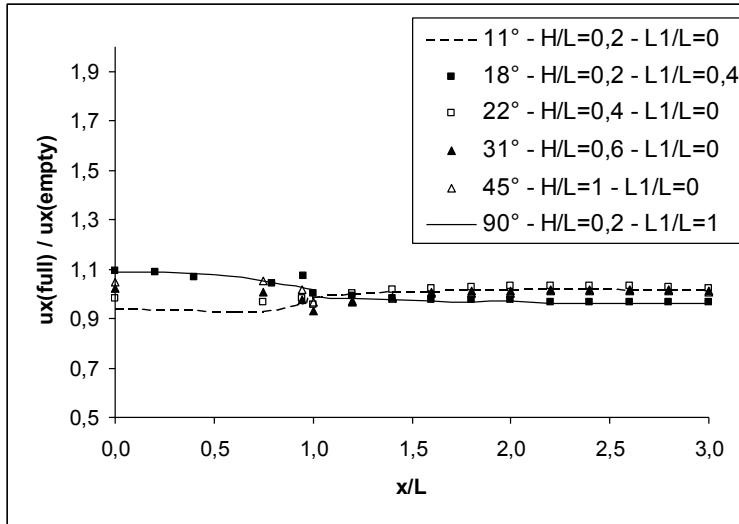


g. u_x , $H/L = 1$, $L_1/L = 0$

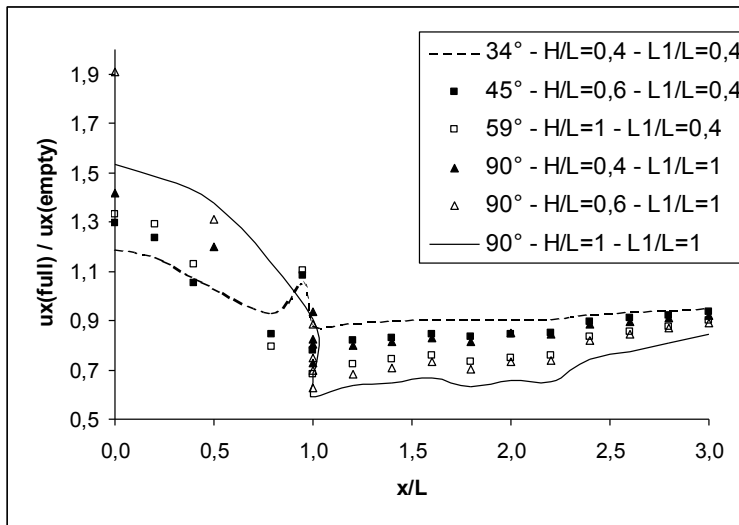


h. u_y , $H/L = 1$, $L_1/L = 0$

Figure 6: Influence of filling on the seismic response of truncated elliptic (a; b; c; d) and elliptic valleys (e; f; g; h)

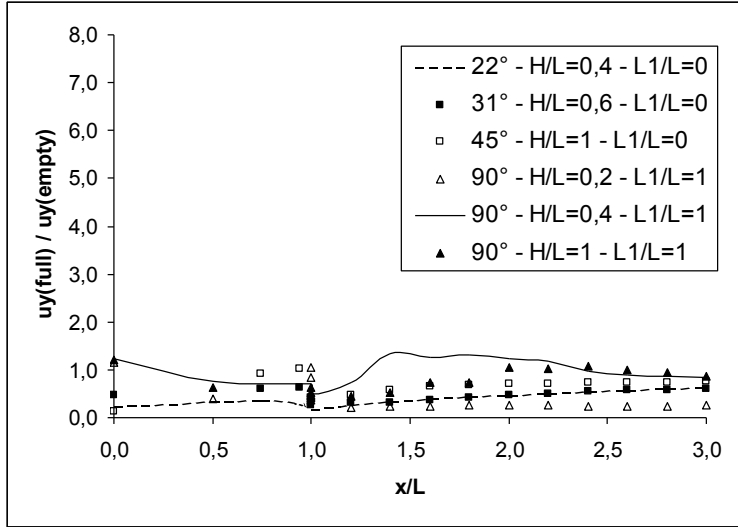


a. Weak 2D geotechnical effects

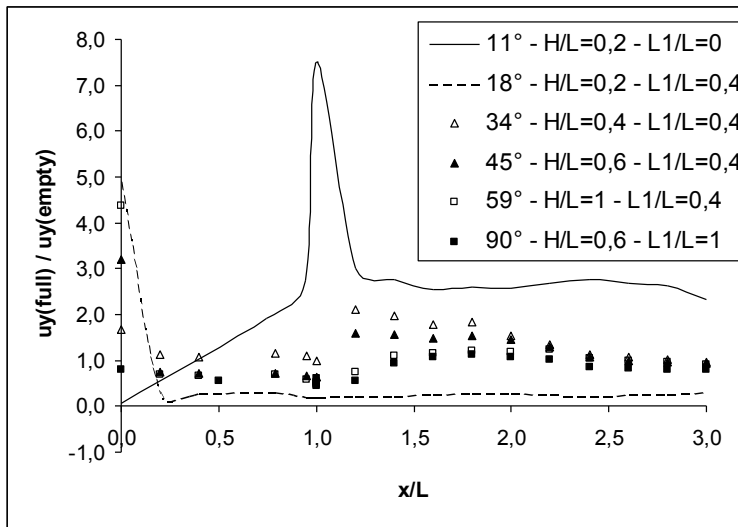


b. Strong 2D geotechnical effects

Figure 7: Characterization of 2D geotechnical effects on horizontal displacements in truncated elliptic valleys



a. Weak 2D geotechnical effects



b. Strong 2D geotechnical effects

Figure 8: Characterization of 2D geotechnical effects on vertical displacements in truncated elliptic valleys

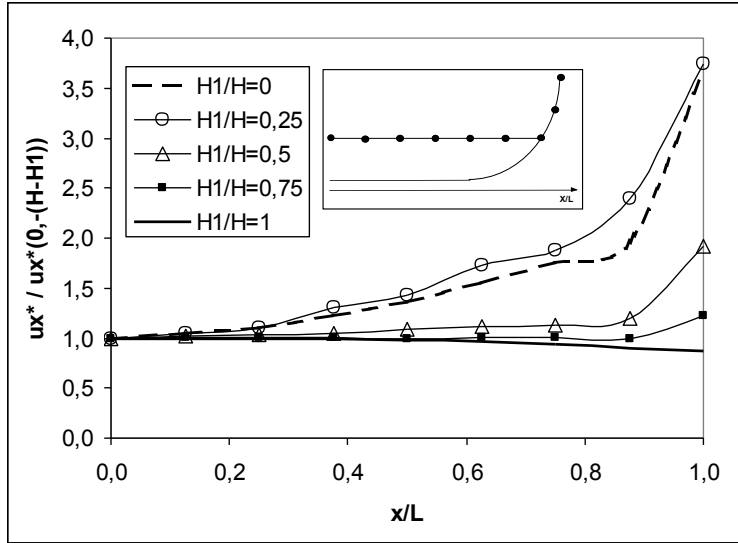


Figure 9: Offset coefficient curves

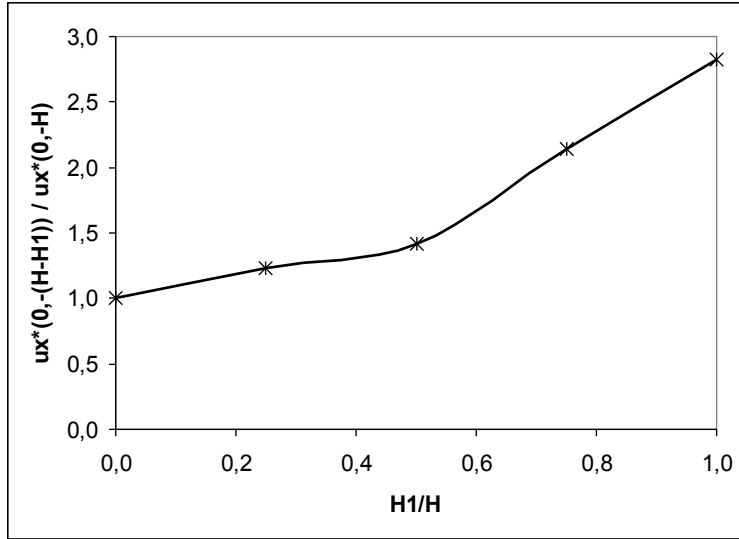


Figure 10: Filling coefficient curve

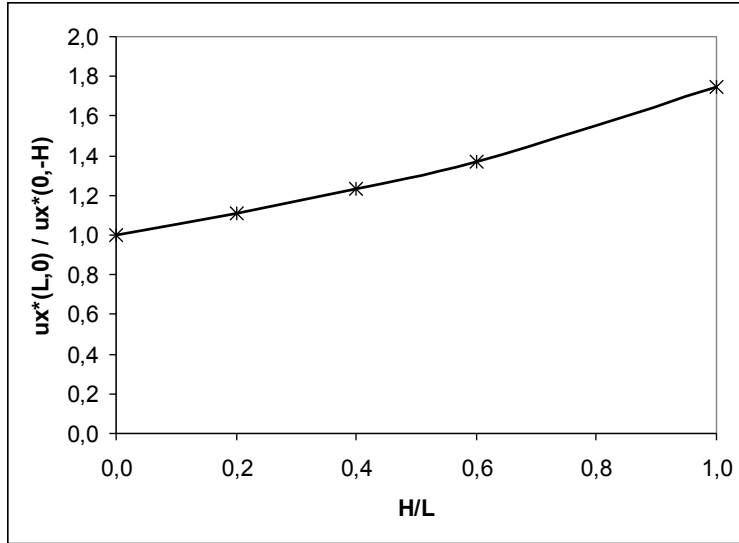


Figure 11: Inversed depth coefficient curve

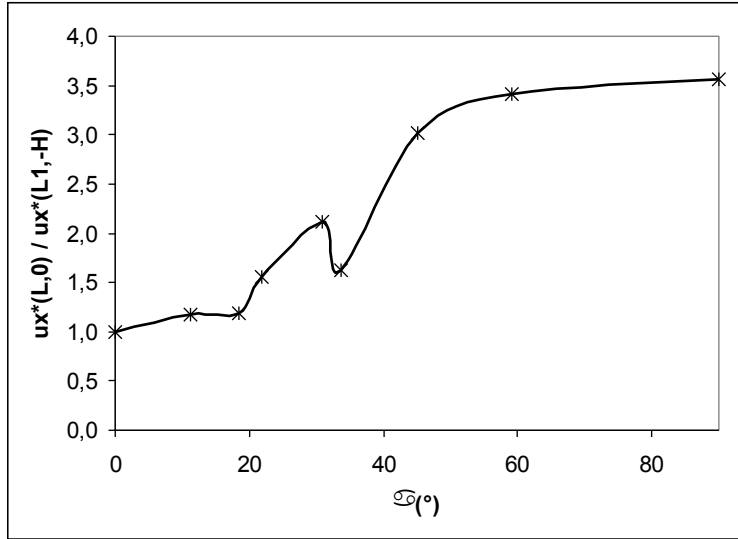


Figure 12: Slope coefficient curve

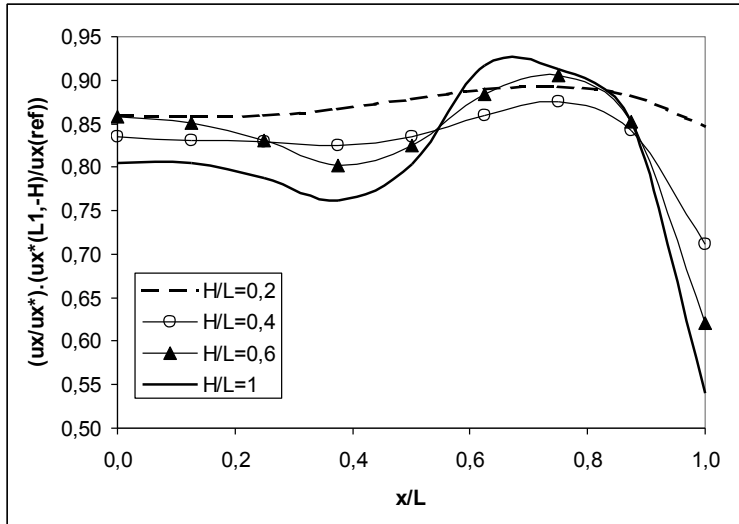
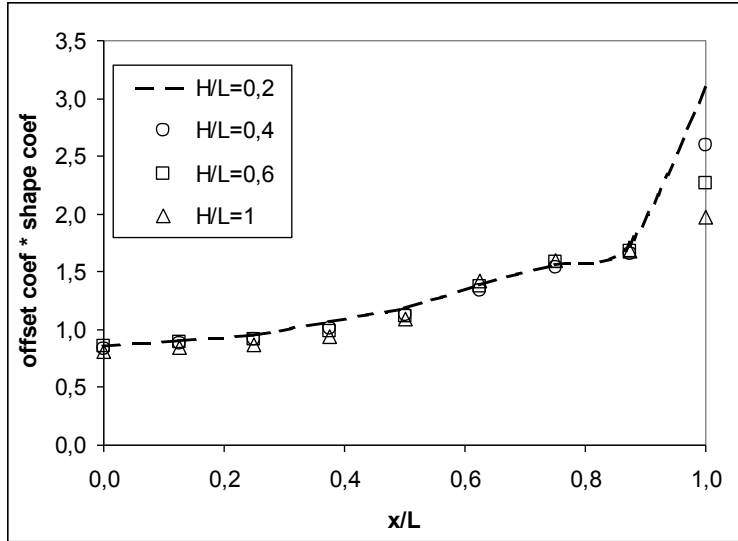
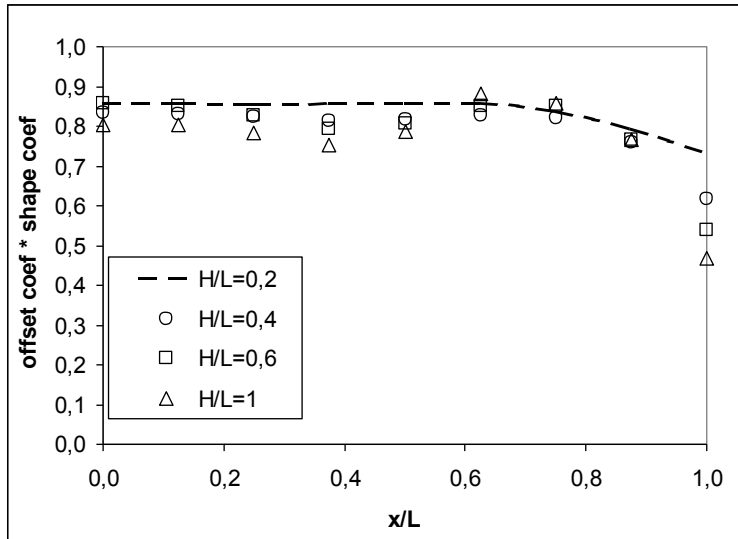


Figure 13: Shape coefficient curves obtained from trapezoidal configurations

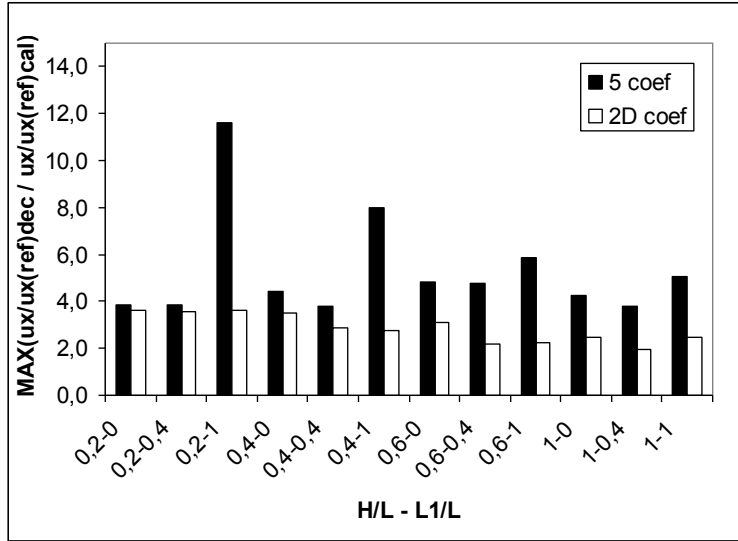


a. $H_1/H = 0$

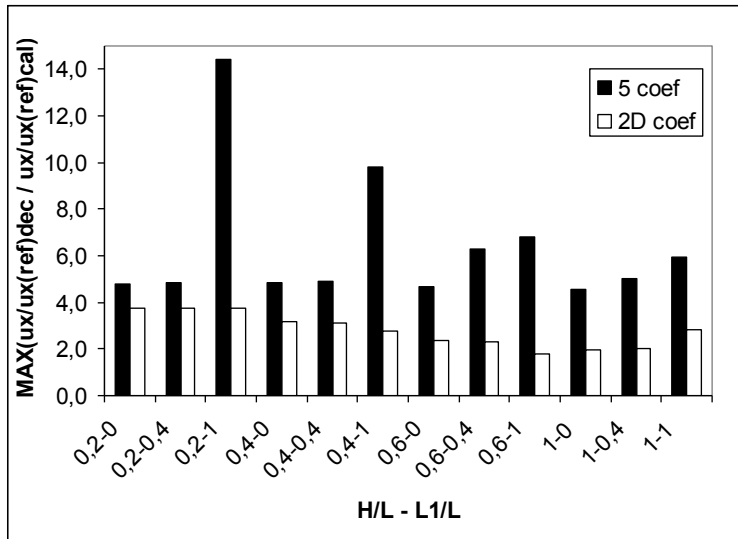


b. $H_1/H = 1$

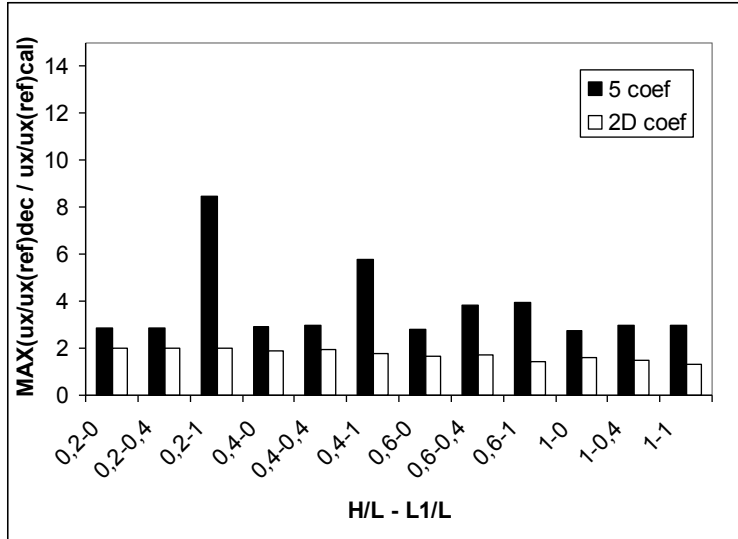
Figure 14: 2DCA coefficients for trapezoidal configurations: empty canyons (a) and full sedimentary valleys (b)



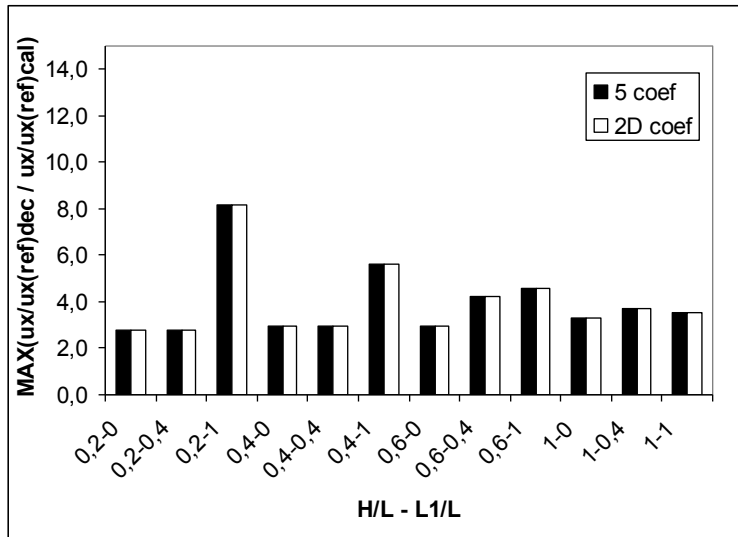
a. $H_1/H = 0$



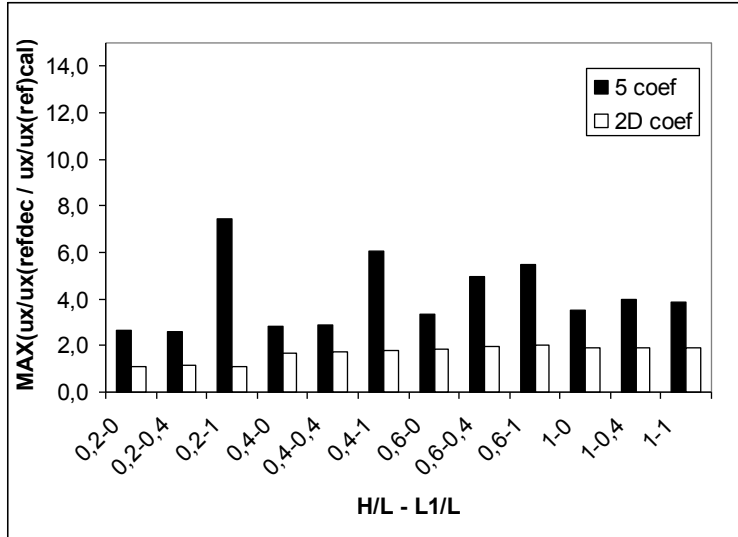
b. $H_1/H = 0.25$



c. $H_1/H = 0.5$

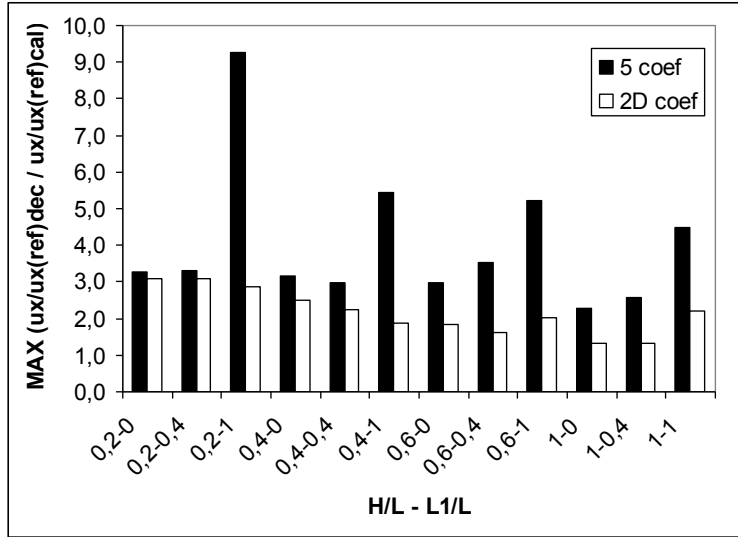


d. $H_1/H = 0.75$

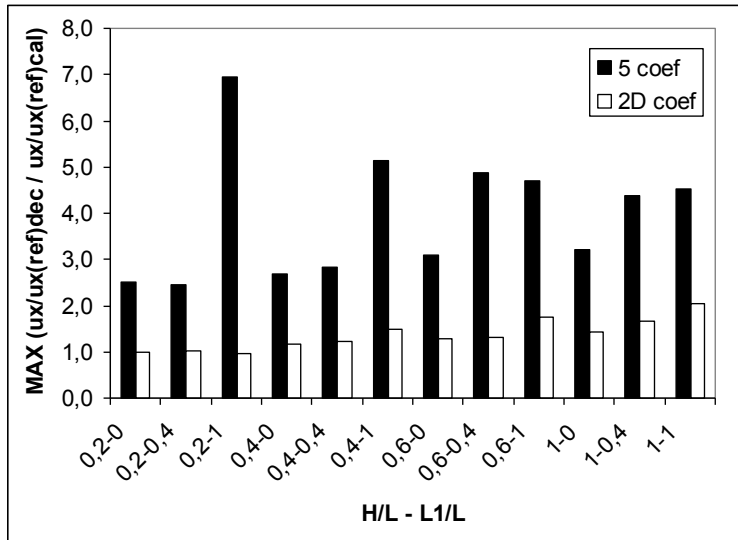


e. $H_1/H = 1$

Figure 15: Maximal values of horizontal surface displacement amplifications provided by both predictive methods for truncated ellipse configurations



a. $H_1/H = 0$



b. $H_1/H = 1$

Figure 16: Maximal values of horizontal surface displacement amplifications provided by both predictive methods for trapezoidal configurations

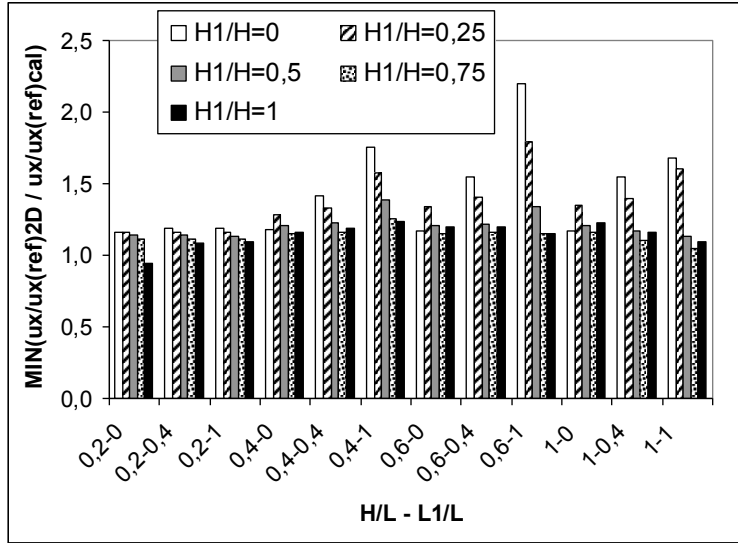


Figure 17: Minimal values of horizontal surface displacement amplifications given by the 2DCA coefficient method in truncated ellipse configurations

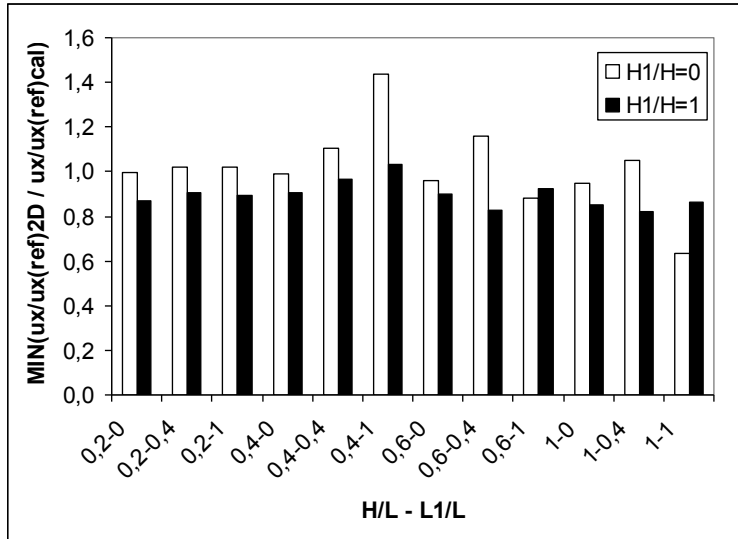


Figure 18: Minimal values of horizontal surface displacement amplifications given by the 2DCA coefficient method in trapezoidal configurations

Table 1: Mechanical parameters of the materials

	E (MPa)	ν	ρ (kg/m ³)	c (m/s)
soil	900	0,3	1630	465
rock	6720	0,4	2450	1000

**Table 2: Values of depth and width at the basis chosen in the parametric studies,
and corresponding values of inclination angle**

L_1/L	H/L			
	0,2	0,4	0,6	1
0	11,31°	21,80°	30,96°	45,00°
0,4	18,43°	33,69°	45,00°	59,04°
1	90,00°	90,00°	90,00°	90,00°

**Table 3: Dependence of 2D geotechnical effects on the inclination angle
(horizontal displacements)**

L_1/L	H/L			
	0,2	0,4	0,6	1
0	11,31°	21,80°	30,96°	45,00°
0,4	18,43°	33,69°	45,00°	59,04°
1	90,00°	90,00°	90,00°	90,00°

**Table 4: 1D fundamental frequencies of the soil columns located at the centre of
the studied valleys**

H_1/H	0	0,25	0,5	0,75	1
H/L=0,2	X	23,24	11,62	7,75	5,81
H/L=0,4	X	11,64	5,82	3,88	2,91
H/L=0,6	X	7,84	3,92	2,59	1,94
H/L=1	X	4,64	2,32	1,55	1,16